



Improved Knock Detection Method Based on New Time-Frequency Analysis In Spark Ignition Turbocharged Engine

Amirhossein Moshrefi^{1*}, Majid Shalchian², Omid Shoaeei¹

¹ School of Electrical and Computer Engineering, University of Tehran (UT), Tehran, Iran

² Department of Electrical Engineering, Amirkabir University of Technology (AUT), Tehran, Iran

ARTICLE INFO

Article history:

Received : 11-May-2018

Accepted: 24-Sep-2018

Published:

Keywords:

Knock effect

Knock sensor

Resonance Frequency

Continues Wavelet Transform

Spark ignition turbocharged engine.

ABSTRACT

One of the main factors that affects outputs, thermal efficiencies and lifetimes of internal combustion engine is “knock effect”. However knock signal detection based on acoustic sensor is a challenging task due to existing of noise in the same frequency spectrum. Experimental results revealed that vibration signals, generated from knock, has certain frequencies related to vibration resonance modes of the combustion chamber. In this article, a new method for knock detection based on resonance frequency analysis of the knock sensor signal is introduced. More specifically at higher engine speed, where there is additional excitation of resonance frequencies, continuous wavelet transform has been introduced as an effective and applicative tool for knock detection and a formula for knock detection threshold based on this method is suggested. Measurement results demonstrate that this technique provide 15% higher accuracy in knock detection comparing to conventional method.

1. Introduction

Auto ignition of air and fuel mixture in combustion chamber due to the increased local temperature and pressure causes the knock phenomena [1]. The occurrence of knock has direct effect on the output power, heat efficiency and gasoline engine lifetime, because it limits the compression ratio and volumetric efficiency and damages engine by creating intensive pressure waves [2-3]. When spark plug ignites, pressure and temperature will be increased in the end of chamber region, air and fuel mixture will be ignited simultaneously and led to pressure oscillation in chamber with high amplitude, in a short time and non-uniform ignition. This event can be identified by several methods, which

divide to direct and indirect categories. Direct method, employs parameters inside the cylinder and indirect method is based on external vibrations. The most accurate sensor for knock detection is the cylinder pressure sensor as a direct method. However, this sensor is expensive and difficult to handle, therefore is only used for calibration during engine tests by dynamometer. Acoustic knock sensors are preferred due to their lower price and installation simplicity, also a single acoustic sensor can detect the knock for all cylinders. However level of noise polluted signal in measurement is higher than cylinder pressure signal [4-5]. Engine noises contain white Gaussian background noise that is generated by the totality of machine events and color noises generated from combustion process, valve

*Corresponding Author
Email Address:

* Corresponding author. E-mail: a.moshrefi@ut.ac.ir

opening, or closing events [6-7]. References [8-11] are applied some filtration approaches to enhance the knock detection on the cylinder pressure sensor. However, these methods have some drawbacks. The first, there is no constant frequency bandwidth for the engine noise and we cannot consider specific frequency region for it, also when noise and signal blend together, this approach cannot be efficient.

References [12-15] have proposed a probability function and noise spectrum estimation. In addition, references [16-19] have introduced some models for the knock event prediction. However, they have used from cylinder pressure signal that it is not commonly applicable in today's automotive industry nor their methods are feasible. References [20-24] have used fast Fourier transform (FFT) or short time Fourier transform (STFT) for knock detection but these methods are not suitable for knock being a non-stationary signal.

In this paper, first we calculate resonance vibration modes for the combustion chamber of EF7 turbo-charged engine, and validate these modes based on measurement data. Then we introduce cross correlation indicator and measure the accuracy of conventional knock detection method based on this indicator. Next, another method for knock detection based on resonant vibration mode analysis is introduced. In the following, continuous wavelet transform, has been presented as the more powerful method for knock detection even at high engine speeds. Finally, the accuracy of these methods has been compared.

2. Cylinder Vibration Frequencies

2.1. Mathematical analysis

Combustion in internal combustion engine is expected to be initiated from spark plug and then spread in all directions. However, sometimes excessive.

temperature and pressure initiates another spark wave which usually moves in opposite direction of main wave front. Due to impact of these wave fronts to combustion chamber walls, unwanted vibrations are occurred inside the cylinder, which lead to pressure oscillations in combustion chamber [4]. In this case, cylinder oscillation frequencies for cylinder with radius of R and height of H, is obtained as the Eq. (1) [25]:

$$F_{m,n,nz} = \frac{C}{2} \sqrt{\left(\frac{\alpha_{m,n}}{R}\right)^2 + \left(\frac{n_z}{H}\right)^2} \quad (1)$$

Where C is the speed of sound, which is approximately 950 m/s for the cylinder. $\alpha_{m,n}$ is vibration mode (m,n) coefficient which is obtained by solving Bessel's equation which has been calculated in advance in [26] and m,n,nz indexes are peripheral, radial and axial frequency mode numbers respectively which have positive or zero values. If $n_z \neq 0$, the mode is known as axial mode and if $n \neq 0$ the mode is known as radial mode and if $m \neq 0$ the mode is known as peripheral mode. Otherwise if only one of the indexes becomes zero, the mode will be known as combination mode [25]. Fig. 1. shows examples of these modes resulted from pressure oscillation effect in combustion chamber.

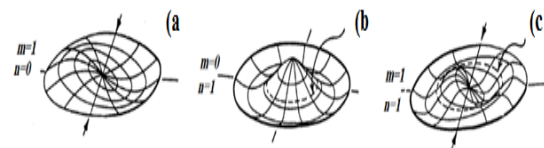


Figure 1: Example of modes, a) Peripheral, b) Radial and c) Combination of radial and peripheral modes. [13]

In the above figure, convex fragment relates to the maximum pressure and concave fragment show the minimum pressure in the combustion chamber. Fig. (1.a) demonstrates peripheral oscillation mode and Fig. (1.b) demonstrates radial oscillation mode. Since cylinder vibration usually occurs near top dead center (TDC), axial vibration mode is negligible and therefore, vibration frequencies can be approximated as Eq. (2):

$$F = \frac{C \cdot \alpha_{m,n}}{2R} \quad (2)$$

2.2. Experimental Verification

For experimental tests an EF7 turbocharged combustion engine with multi point port fuel injections has been installed on AVL dynamometer type APA 1F4-E-0509 with the maximum power of 220 kW. Internal pressure of each cylinder was measured and recorded with AVL GH12D pressure transducers and used as a reference for knock detection. Also Siemens VDO 5WY2414A knock sensor has been mounted on

Improved Knock Detection Method Based on New Time-Frequency Analysis In Spark Ignition Turbocharged Engine

the engine block. Data from all of these sensors have been recorded at the same time. Some of engine characteristics are provided in Table 1. Tests have been performed on this engine with 95 octanes petroleum fuel.

Now from Table 1. and Eq. (2), we can predict knock resonant frequencies. Table 2. shows vibration coefficients and resonant frequencies for three peripheral modes, one radial mode and one combination mode. Positive and negative signs, in mode shape, illustrate the area with above average and below average pressure inside the chamber. These modes are sorted from minimum to maximum frequency in ranges.

Table 1: Table caption (Times New Roman 10 regular)

Description	Value	Unit
Engine Model	EF7 turbocharged	-
	, gasoline	
Displacement	1.646	L
Bore * Stroke	78.6*85	mm
Compression Ratio	9.5	-
Gasoline injection pressure	3.5	bar
No. of cylinders	4 (in-line)	-

Table 2. Knock vibration modes in combustion chamber and related coefficients and frequencies

m,n	a(1/0)	b(2/0)	c(0/1)	d(3/0)	e(1/1)
Mode Shape					
$\alpha_{m,n}$	0.586	0.972	1.220	1.337	1.697
$f_{m,n}(\text{kHz})$	7.141	11.845	14.867	16.292	20.679

In above Table, mode a(1/0) is the vibration mode with peripheral mode 1 and radial mode 0 which is the first vibration mode with 7.141 (kHz) frequency and mode c(0/1) is the vibration mode with peripheral mode 0 and radial mode number 1 which is third vibration mode with 14.876 (kHz) resonant frequency.

Based on the mathematical analysis, it is expected to observe knock signal in frequency domain as peaks at vibration modes specified in Table 2. Fig.

2 demonstrates two experimental output data of knock sensors with and without knock condition. Red window specifies knock sampling window which is engine phase synchronized window for a specific cylinder. Frequency spectrums for these two signals are shown in Fig. 3.

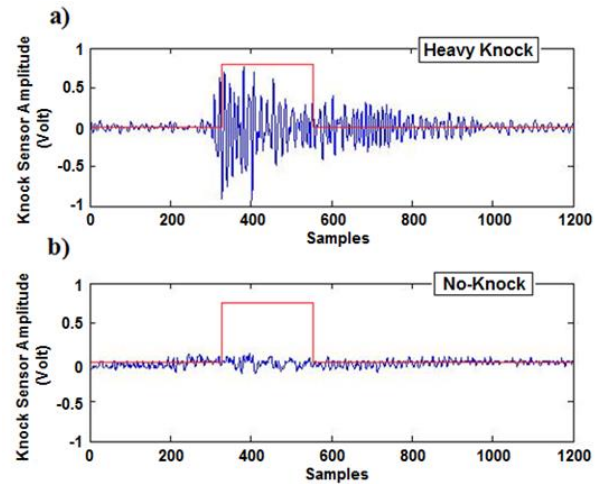


Figure 2: a) Sensor signal with knock condition b) Sensor signal without knock condition both for engine speed of 3500 rpm and engine load of 125%.

As depicted in Fig. (3.a), under knock condition, knock resonance frequencies are clearly appeared for a, b, c modes introduced in Table 2. This result verifies mathematical analysis of knock resonance frequencies

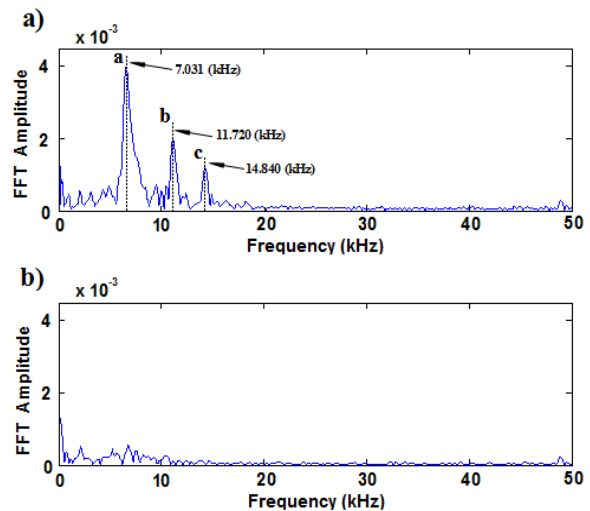


Figure 2: Frequency spectrum of sensor signals a) With knock, b) Without knock

3. Knock Detection Method

3.1. Conventional Method

Fig. 4 demonstrates block diagram of conventional knock detection method, including four components. First the obtained signal from

knock sensor is amplified, then this signal passes through a band pass filter and a full wave rectifier and finally the signal intensity is

summed up by using an integrator block. The result of accumulated signal intensity is compared with a threshold to detect the knock occurrence [27].

$$C = \frac{N \sum_{i=1}^N x(i)y(i) - \sum_{i=1}^N x(i) \sum_{i=1}^N y(i)}{[(N \sum_{i=1}^N x^2(i) - (\sum_{i=1}^N x(i))^2) * (N \sum_{i=1}^N y^2(i) - (\sum_{i=1}^N y(i))^2)]^{1/2}} \quad (3)$$

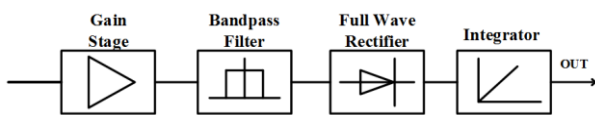


Figure 4: Block diagram of conventional knock detection method

To study the accuracy of this method cross correlation (CC) indicator is defined as Eq.

Where x and y are the determined intensity from knock sensor and cylinder pressure sensor respectively and N is the number of measurement cycles. As mention earlier the cylinder pressure sensor detects the knock with very high accuracy, therefore knock intensity from this sensor is selected as the reference, and accuracy of knock detection based on conventional method is measured based on cross correlation with this reference. For knock intensity calculation from pressure sensor data, at first the band-pass filter from 4 to 40 kHz for the cylinder pressure signal is calculated. After that, the filtered signal is rectified and the integration value of the rectified signal in a definite window, i.e. 0-90 CA after TDC, is the knock intensity of each engine cycle.

Engine load of 125%. Average cross correlation for all cylinders is 67%.

3.2. New method based on Time-Frequency analysis

Conventional method has several weaknesses; first the band pass filter is far from ideal filter and attenuates the signal level in resonant mode A and C. Also it is well known that the destructive effect of knock is the result of recurring oscillations, however conventional method integrates the signal intensity over the whole time period of

knock window and it does not consider that how long in the time domain, the specific frequency has been repeated. Therefore conventional method cannot identify destructive knock signals. The first weakness can be resolved by applying FFT and analyzing the signal in frequency domain and in the range of resonance vibration mode, But FFT method cannot decrease noise in signal band. In other word conventional method and Fourier transform method is not the right tool to study non-stationary signals such as cylinder vibrations.

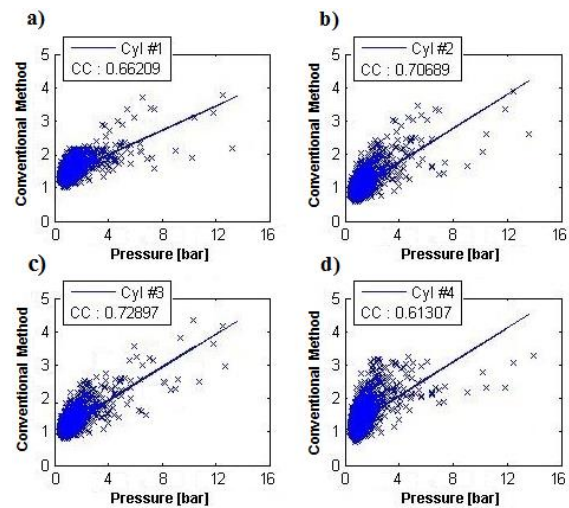


Figure 5: Cross correlation of knock intensity for conventional method and cylinder pressure sensor data for 2200 cycles at engine speed of 5800 rpm and engine load of 125%. a) Cross correlation for cylinder #1 b) Cross correlation for cylinder #2 c) Cross correlation for cylinder #3 d) Cross correlation for cylinder #4.

3.2.1. Short-time Fourier Transformation (STFT)

For non-stationary signals, the signal can be divided into sufficiently small sections and those sections can be considered as stationary. For this purpose, a window function w(t) is used to divide the sections of signal. Thus, STFT of signal x(t) is defined as follows [28]:

$$STFT_x^W(\tau, f) = \int_{-\infty}^{+\infty} x(t)W^*(t-\tau)e^{-j2\pi ft} dt \quad (4)$$

Where f is the frequency domain variable and τ is the time domain variable.

3.2.2. Wavelet transformation

Improved Knock Detection Method Based on New Time-Frequency Analysis In Spark Ignition Turbocharged Engine

Window function, which is used in STFT, has fixed dimensions. Therefore, all segments have similar resolution. However, it would be preferred to choose the length of the window for optimized non-uniform resolution in time and frequency domains, while maintaining the stationary segments. So another transform is proposed with variable resolution that is called wavelet transform.

3.2.3. Continuous Wavelet Transformation (CWT)

To implement variable resolution, width of the window varies along with the frequency components. Continuous wavelet transform is defined as follow [29]

$$CWT_x^\psi = \Psi_x^\psi(\tau, s) = \frac{1}{\sqrt{|s|}} \int_{-\infty}^{+\infty} x(t) \cdot \psi^* \left(\frac{t-\tau}{s} \right) dt \quad (5)$$

Where τ and s are the time and scale variables respectively and Ψ is the window function called “mother wavelet” because it is the template function for production of other windows. The scale variable has reciprocal relationship with frequency.

Fig. 6 shows resolution plane for various transformations on time, frequency, and time-frequency planes. This figure indicates that because of constant window in STFT, uniform resolution is created around the time-frequency plane. While in CWT, length and width of the rectangular sections vary, however the area is fixed. In other word, each rectangular section is a member of time-frequency plane, locates in specific place in time and frequency domains. In wavelet transform, larger scales (lower frequency), have shorter height which correspond to the higher resolution. It is interesting to note that major resonance modes of knock vibrations occurred in lower frequency range and this is coordinated with characteristics of wavelet transform that provide higher resolution at lower frequency ranges.

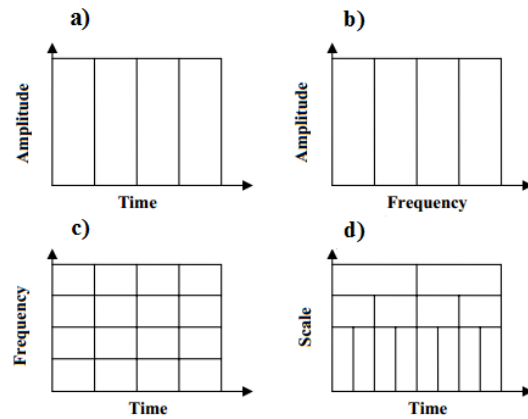


Figure 6: Resolution planes for different transformations. (a) Time plane, (b) frequency plane, (c) STFT time-frequency plane, (d) CWT time-frequency plane [29]

3.3. Conceptual model for CWT

The relation of CWT can be written as inner product of signal and a basic function as Eq. (6) [30-31]

According to the above equation, CWT is a measure of the similarity between the signal and the basic function. In other word, CWT coefficients describe that how the signal is similar to the wavelet in the specified scale. For example, if signal has a prominent frequency component in the scale, then the scaled wavelet would be similar to the target signal and therefore, coefficient of CWT at this scale, will be relatively large.

4. Results and Discussion

Fourier transform of the signal implies the number of occurrence of each frequency, however in the presence of background noise, or at high engine speed, FFT method show weakness and cannot identify the signal from background noise.

4.1. Strong Background Noise

Since the noise of engine vibration has a random nature, it does not have prominent frequency component in a signal frequency band. This can be observed by comparing between power spectrum of knock sensor signal under normal combustion and considerable noise as shown in Fig. (7.a) and power spectrum of knock sensor with knock condition as shown in Fig. (7.b).

Fig. (7.b) shows clear peaks at expected knock resonance frequencies, while Fig. (7.a) shows only random fluctuations.

4.2. High Engine Rotation Speed

Excitation of resonance vibration frequencies at high engine speed is another important factor which limits the performance of Fourier transformation method. Fig. 8 shows two cylinder pressure sensor data at engine speed of 5800 rpm.

For signal shown in Fig. (8.a) knock intensity is equal to 3.8 bar while for signal in Fig. (8.b) knock intensity is 7.9 bar, which means the existence of knock in case (8.b). Frequency spectrum of the Fourier transform for these two

signals is demonstrated in Fig. 9 which does not show significant difference.

Also Fig. 10 shows STFT of the two signal above mentioned which does not demonstrate meaningful difference and cannot detect knock event.

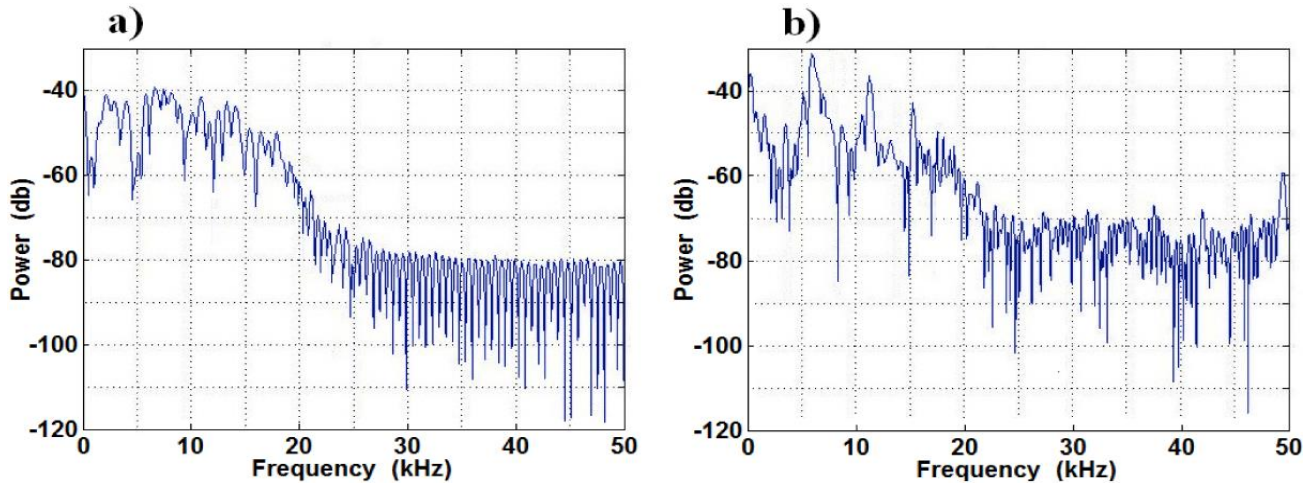


Figure 7: Power spectrum of knock sensor signals: a) Normal combustion with noise. b) Combustion with knock.

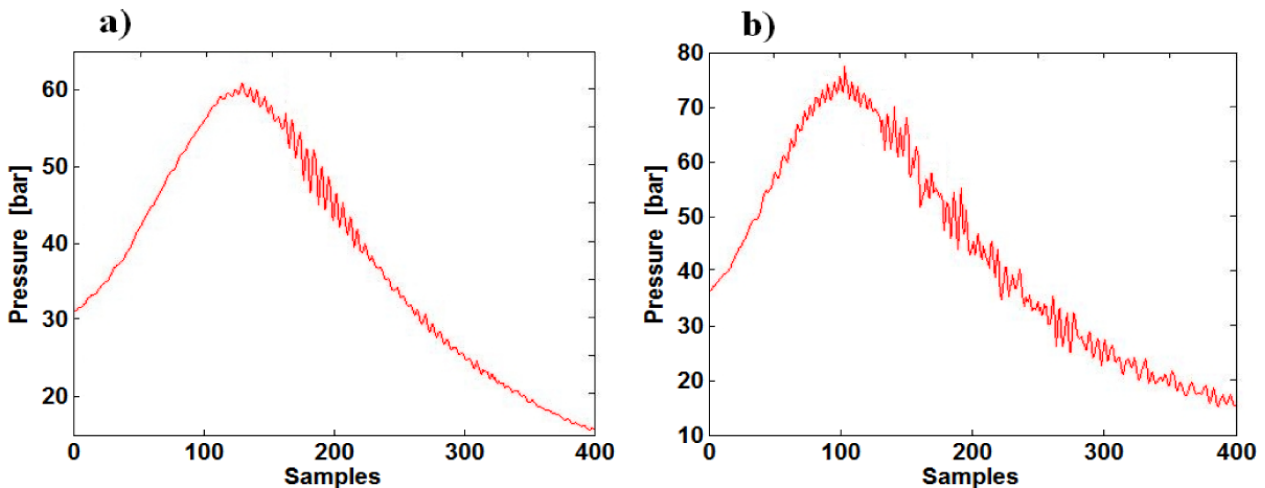


Figure 8: Cylinder pressure sensor data at engine speed of 5800 rpm and load of 125% a) Normal combustion b) Combustion with knock

Improved Knock Detection Method Based on New Time-Frequency Analysis In Spark Ignition Turbocharged Engine

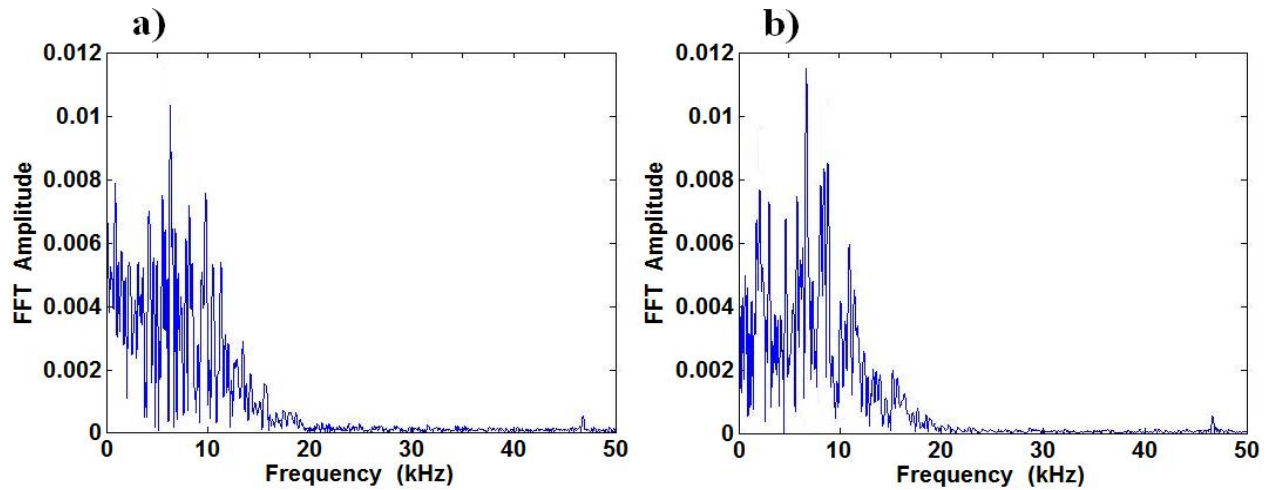


Figure 9: Frequency spectrums of Fourier transform a) Signal of Fig (8.a) and b) Signal of Fig (8.b)

Thus by adjusting the threshold level, only the sum of prominent coefficients of the CWT are taken into account and product of these wavelet coefficients in summation of the frequency spectrum can be introduced as an indicator for knock detection.

This new indicator for determination of knock intensity (KI) is summarized in Eq (7).

$$KI = \begin{cases} (1 + \sum_{\tau_i} \sum_{s_i} CWT) \cdot (\sum_{f_1}^{f_2} fft); & CWT(\tau_i, s_i) > THR \\ \sum_{f_1}^{f_2} fft; & O.W \end{cases} \quad (7)$$

Where τ_i and s_i specify segments for which CWTs are higher than the threshold limit. So if there are some

segments with prominent CWT coefficient, their effect magnifies in knock intensity by a multiplicative coefficient, otherwise only simple summation is used to calculate knock intensity as previous method.

Cross correlation of estimated knock intensity based on CWT method to the reference with threshold value of 0.2 and frequency range of 6-15 kHz at engine speed of 5800 rpm and engine load of 125% has been shown in Fig. 12 for all four cylinders.

It can be observed that CWT method improves knock detection accuracy. Average cross correlation increased from 67% to 78% which means 15% higher detection accuracy.

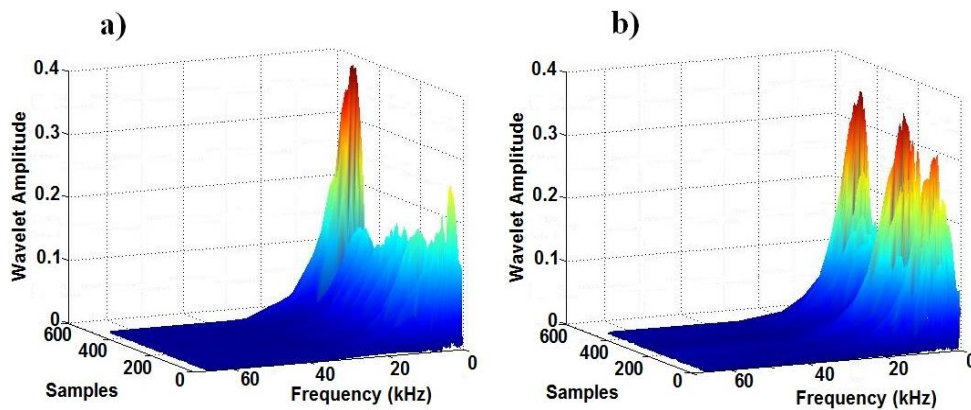


Figure 11: Spectrum of the CWT, respectively. a) Signal from Fig. (8.a), and b) Signal from Fig. (8.b)

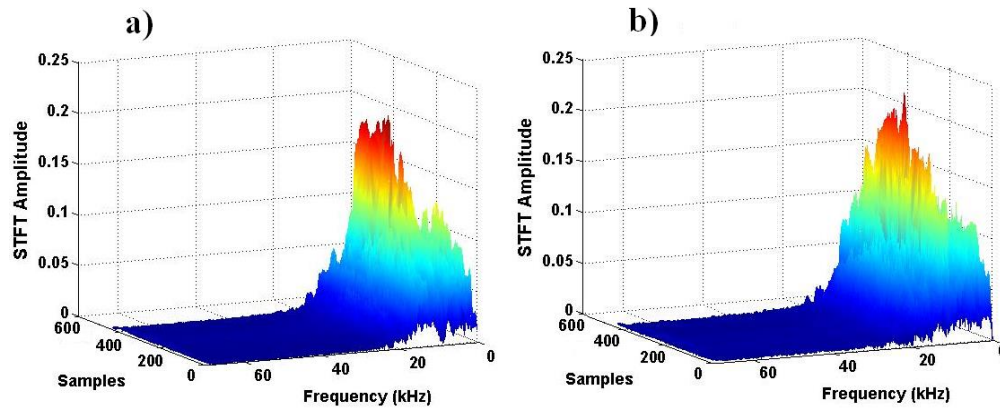


Figure 10: Power spectrum of knock sensor signals: a) Normal combustion with noise. b) Combustion with knock.

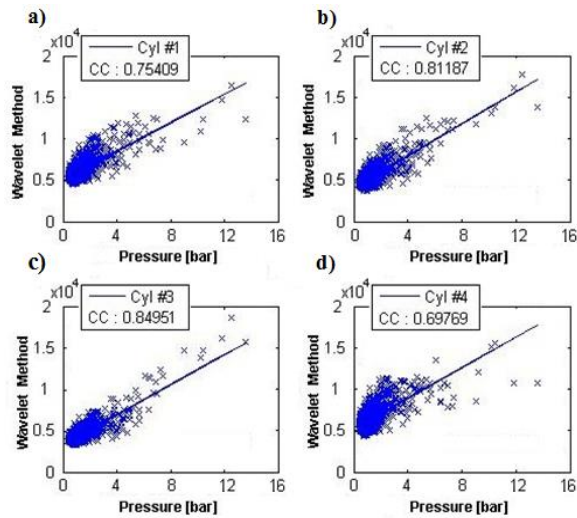


Figure 12: Cross correlations of CWT method intensity to the reference for engine speed of 5800 rpm and engine load of 125% for four-cylinders. a) Cross correlation for cylinder #1 b) Cross correlation for cylinder #2 c) Cross correlation for cylinder #3 d) Cross correlation for cylinder #4.

Table 3. Cross Correlation of the knock intensity to the reference for three knock detection methods

Cylinder #	Methods Convolutional Method	FFT Method	Proposed Method
1	0.66209	0.68124	0.75409
2	0.70689	0.74372	0.81187
3	0.72897	0.76107	0.84951
4	0.61307	0.63547	0.69769
Average CC	0.67	0.71	0.78

Table 3. summarizes the result of cross correlation to the reference for three mentioned methods for all four cylinders. It should be noted the accuracy of detection is always lower in cylinder 1 and 4 since those cylinders have larger distance from knock sensor comparing to their pairs.

5. Conclusion

In this paper, first we have calculated resonance vibration modes of the cylinder for EF7 engine. Measurement data confirms that in case of knock occurrence there is strong signal intensity around those vibration modes and this feature has been used to improve the accuracy of knock detection. Results of intensity from cross

Improved Knock Detection Method Based on New Time-Frequency Analysis In Spark Ignition Turbocharged Engine

correlation indicator, suggested that accuracy of knock estimation improves 6% comparing to the conventional method. To improve further the accuracy of knock detection, especially under noisy environment or at high engine speed, another method based on continuous wavelet transform has been introduced. Test results of this method indicate that accuracy improves around 15% comparing to conventional method.

References

- [1] J.B. Heywood; Internal combustion engine fundamentals, McGraw-Hill Book Company, New York, (1988).
- [2] M. Castagne, et al; New knock localization methodology for SI engines, SAE transactions 112.3: 1584-1594, (2003).
- [3] G.D. Errico, et al; Application of a thermodynamic model with a complex chemistry to a cycle resolved knock prediction on a spark ignition optical engine, International Journal of Automotive Technology 13.3: 389-399, (2012).
- [4] D. Kjellqvist; Concepts, strategies and controller for gasoline engine management, Diss. MSc thesis. Lulea University of Technology, Sweden, (2005).
- [5] JCP. Jones, J. Frey, and S. Shayestehmanesh. "Stochastic simulation and performance analysis of classical knock control algorithms." IEEE Transactions on Control Systems Technology 25, no. 4: 1307-1317, (2017).
- [6] JCP. Jones, J. Frey, and S. Shayestehmanesh. "Stochastic simulation and performance analysis of classical knock control algorithms." IEEE Transactions on Control Systems Technology 25, no. 4: 1307-1317, (2017).
- [7] C. Hudson, X. Gao, and R. Stone; Knock measurement for fuel evaluation in spark ignition engines, Fuel 80.3: 395-407, (2001).
- [8] E. Galloni, G. Fontana, and S. Staccone; Numerical and experimental characterization of knock occurrence in a turbo-charged spark-ignition engine, Energy Conversion and Management 85: 417-424, (2014).
- [9] K. Kim, M. Szedlmayer, K. Kruger, and C. Kweon; Optimization of In-Cylinder Pressure Filter for Engine Research, No. ARL-TR-8034. US Army Research Laboratory Aberdeen Proving Ground United States, (2017).
- [10] Z. Wu, and S. Naik; DSP Applications in Engine Control and Onboard Diagnostics: Enabling greener automobiles, IEEE Signal Processing Magazine 34. 2: 70-81, (2017).
- [11] J. Vavra, et al; Knock in Various Combustion Modes in a Gasoline-Fueled Automotive Engine, Journal of Engineering for Gas Turbines and Power, 134.8: 082807, (2012).
- [12] J. Ghandhi, and K. Kim; A Statistical Description of Knock Intensity and Its Prediction, No. 2017-01-0659. SAE Technical Paper, (2017).
- [13] A. d'Adamo, S. Breda, S. Fontanesi, A. Irimescu, S. Silvia Merola, and C. Tornatore; A RANS knock model to predict the statistical occurrence of engine knock, Applied Energy 191: 251-263, (2017).
- [14] T. Ibuki, et al; Knocking detection in gasoline engines based on probability density functions: A mixed Gaussian distribution approach, 2015 54th IEEE Conference on Decision and Control (CDC). IEEE, (2015).
- [15] A. D'Adamo, S. Breda, S. Iaccarino, F. Berni, S. Fontanesi, B. Zardin, M. Borghi, A.

Irimescu, and S. Merola; Development of a RANS-Based Knock Model to Infer the Knock Probability in a Research Spark-Ignition Engine, SAE International Journal of Engines 10, no. 2017-01-0551, (2017).

[16] T. Li, T. Yin, and B. Wang; A phenomenological model of knock intensity in spark-ignition engines, Energy Conversion and Management 148: 1233-1247, (2017).

[17] I. Tougri, J. Marcelo, A. Leiroz, and T. Melo; Knocking prediction in internal combustion engines via thermodynamic modeling: preliminary results and comparison with experimental data, Journal of the Brazilian Society of Mechanical Sciences and Engineering 39, no. 1: 321-327, (2017).

[18] C. Netzer, L. Seidel, M. Pasternak, C. Klauer, C. Perlman, F. Ravet, and F. Mauss; Engine Knock Prediction and Evaluation Based on Detonation Theory Using a Quasi-Dimensional Stochastic Reactor Model, No. 2017-01-0538, SAE Technical Paper, (2017).

[19] K. Siokos, Z. He, and R. Prucka; Assessment of Model-Based Knock Prediction Methods for Spark-Ignition Engines, No. 2017-01-0791, SAE Technical Paper, (2017).

[20] Y. Sugure, et al; Virtual Engine System Prototyping with High-Resolution FFT for Digital Knock Detection Using CPU Model-Based Hardware/Software Co-simulation, SAE International Journal of Passenger Cars-Electronic and Electrical Systems 2.2009-01-0532: 177-185, (2009).

[21] A. Taghizadeh-Alisarai, et al; Characterization of engine's combustion-vibration using diesel and biodiesel fuel blends by time-frequency methods: A case study, Renewable Energy 95: 422-432, (2016).

[22] S. d'Ambrosio, A. Ferrari, and L. Galleani; In-cylinder pressure-based direct techniques and time frequency analysis for combustion diagnostics in IC engines, Energy Conversion and Management 99: 299-312, (2015).

[23] F. Omar, M. Selim, and S. Emam; Time and frequency analyses of dual-fuel engine block vibration, Fuel, 203: 884-893, (2017).

J. Ladd, D. Olsen, and G. Beshouri; Evaluation of operating parameters and fuel composition on knock in large bore two-stroke pipeline engines, Fuel 202: 165-174, (2017).

[24] T. Bengisu; Computing The Optimum Knock Sensor Locations, SAE International, Paper No. 2002-01-1187, (2002).

[25] D. Siano, et al; The Use of Vibrational Signals for On-Board Knock Diagnostics Supported by In-Cylinder Pressure Analyses, No. 2014-32-0063. SAE Technical Paper, (2014).

[26] A. Stotsky; Automotive Engines: Control, Estimation, Statistical Detection, 2009 edition, Springer, (2009).

[27] A. Oppenheim, R. Schaffer, J. Buck; Discrete-Time Signal Processing, 3rd Edition, Prentice Hall, (2009).

[28] D. Walnut; An Introduction to Wavelet Analysis, 2nd Edition, Springer, (2007).

[29] D. Hong, J. Wang, R. Gardner; Real Analysis with an Introduction to Wavelet and Applications, 1st Edition, Elsevier, (2008).

[30] L. Debnath, and A. Firdous, Lecture Notes on Wavelet Transforms. Springer International Publishing, (2017).